

~~FILE COPY~~  
NO. 2

FILE COPY  
NO. 1-W

CASE FILE  
COPY

TECHNICAL MEMORANDUMS

NATIONAL ADVISORY COMMITTEE FOR AERONAUTICS

---

No. 511

---

ON THE STRENGTH OF BOX TYPE FUSELAGES

By J. Mathar

From the 1928 Yearbook of the  
Wissenschaftliche Gesellschaft für Luftfahrt

FILE COPY

To be returned to  
the files of the National  
Advisory Committee  
for Aeronautics  
Washington, D. C.

---

Washington  
May, 1929

FILE COPY

To be returned to  
the files of the National  
Advisory Committee  
for Aeronautics  
Washington, D. C.

NATIONAL ADVISORY COMMITTEE FOR AERONAUTICS.

TECHNICAL MEMORANDUM NO. 511.

ON THE STRENGTH OF BOX-TYPE FUSELAGES.\*

By J. Mathar.

The behavior of thin-walled box girders is a frequently recurring question in technical practice. It has often been treated theoretically, but only in a few cases, experimentally. Still, the complete investigations cover the stress conditions of box-girder walls below the buckling load. As regards the buckled condition, only the buckling stress has been determined experimentally and by calculation. Conditions grow very intricate, when girders consist of members lying partly above and partly below the buckling stress, as do many spar and most wing and fuselage structures in airplane construction. One has to resort to tests and especially to tests within the elastic limit, in order to gain an idea of the deformations and stresses developed in such structures.

The present investigation relates to a box-type fuselage with sides consisting of thin smooth sheet metal, stiffened by longitudinal members riveted to the flanged channel-section bulkheads or transverse frames and to the semicircular corrugated corner stiffenings. The results obtained in this particular case can be applied to a great number of similar structures.

The maximum load adopted for the tests was such that no permanent

\*"Ueber die Festigkeit von Kastenrumpfen," from the 1928 Yearbook of the Wissenschaftliche Gesellschaft für Luftfahrt, pp. 105-109.

deformation could be found at any point with the measuring instruments used.

The inverted fuselage was secured to a heavy supporting stand (Figure 1) at the points of attachment of the wings and struts and remained in the same position during all the tests.

The stand was placed on a heavy foundation, in order to enable the stresses developed by the tests and especially by the vibrations of the fuselage to be absorbed with the least possible displacement of the plane of fixation.

All the tests were divided into two groups: the first, dealing with static investigations and the second with vibrational phenomena. The static investigations were made separately for the bending about the beam and the vertical axis and for the torque. The investigation dealing with the vibrational phenomena covers the two bending vibrations and the torsional vibrations in conjunction with the static investigations. For lack of time, I shall be able to take up only the most essential points.

The loading for the bending of the fuselage about the beam axis was effected by a single force, acting at the tail end. This loading was produced by a hydraulic jack or, when it had to remain strictly constant for a long time, by weights conjunctly with a jack. The hydraulic device produced a maximum load of 750 kg (1653 lb.). Up to this load, all the measured stresses and deformations were almost exactly proportional to the loading.

An accurate proportionality was prevented by the small local deflections which invariably arose, especially in the covering, during the assembly of the light sheet and section member structures. These deflections were smoothed out with increasing load and only then admitted an accurate proportionality between deformation and loading. In the present case this difference was very small, since there were no marked local distortions in the covering.

The measured deflection curve of the fuselage for a load of 300 kg (661 lb.) is shown in Figure 2. The calculated deflection curve is likewise plotted in the same figure under the assumption that the stress is distributed linearly over the cross section. A comparison of the two curves shows that in each cross section the measured deflections are greater than the calculated ones and that the difference increases with increasing participation of the sheet metal in the moment of inertia.

The stresses were determined for the longitudinal members and the corner stiffenings both on the tension and on the compression side, at the points presumably most highly stressed. Only the elongations in one direction were measured for the determination of the stresses, whence, by means of the modulus of elasticity, it was inferred that a stress was acting in this direction. It follows from the measurement (Figure 2) that the average stress is  $100 \text{ kg/cm}^2$  (205,000 lb./sq.ft.) for a load of 300 kg (661 lb.), that it is much better balanced in tension

than in compression and that it decreases toward the tail end. A thorough investigation of the variable-stress curve on the compression side shows that the behavior of the stress is periodical in each bay. It falls below the mean value at the two transverse frames, rises above it toward the center and at this point again drops below the mean value.

For the sake of obtaining a good insight into the conditions of deformation, in order to determine the type and magnitude of the effect of the different components, the total deflection of the structure and of the covering was determined for several bays bounded by two frames. The results of these tests are shown in Figure 3. The total distortions for a load of 300 kg are plotted with relation to the rear bulkhead, which is considered as fixed.

The deformations, which seem very intricate at first sight, are considerably simplified by a comparison with those of a box with rigid corners, as shown in Figure 4. The right angles at the corners of this box are not affected by the deformation. The upper strip, which works in compression, buckles, while the lower one, which works in tension, tends to stretch.

The differences between the fuselage structure and this box are primarily due to the sheet-metal covering. Thus the two upper longitudinal members, which work in compression, are again pressed outward in the center between two frames. This additional curvature is accounted for by the fact that the upper

sheet is not compressed but is bent outward and tends to pull the longitudinal section member along with it. The sheet could as well bend inward as outward, but the outward bend is favored by the riveting method and by the position of the sheet under normal conditions. The above-mentioned curvature of the longitudinal sections likewise accounts for the periodical stress distribution, as illustrated by Figure 2. The behavior of the upper corner stiffeners is still more intricate, since the influence of the side sheets must likewise be added to the influence of the upper sheet and of the fixed riveting at the frames.

In connection with the displacement of the supporting frame the side sheets are stretched diagonally and form corrugations, as shown in Figure 5. The points of equal curvature are represented by the closed lines. In the present case the curvature is inward. The reasons are similar to those previously mentioned for the upper sheet.

On account of the corrugation of the side sheets the lateral shank of the corner stiffeners bends inward and hence, necessarily produces a stronger outward pressure in the center of the upper shank than in the case of the longitudinal sections.

The behavior of the longitudinal bottom sections and corner stiffeners, which/<sup>work</sup>in tension, is similar to that of the upper ones. However, their deformations, and hence their stresses, are better balanced, since the compressive or buckling stresses are replaced by tensile stresses.

The moment of inertia of the fuselage can be calculated approximately from the aforesaid behavior of the fuselage components. The test showed that the moments of inertia determined with the total cross section must necessarily have been too large and hence the deflections too small (Figure 6a), since the sheet, working under compression, has scarcely any bearing capacity, while the side sheets are less favorably stressed than is assumed for the calculation with a linear stress distribution. When, in the calculation of the moment of inertia, the top and side sheets are entirely neglected, it appears that, according to the aforesaid test results, the moments of inertia must be too small and hence the deflections calculated with the moments must be too large. When only the top sheet is neglected, the calculated deflection line must lie between the measured line and the line calculated for the total moment of inertia (Figure 6b). A closer approximation is afforded by entirely neglecting the top sheet and taking the side sheet at only half its value. The side sheet is introduced at only half its value, since it can only work in tension on account of its low bending strength. The moment of inertia, obtained from these values, yields a deflection line which agrees sufficiently well with the measured line (Figure 6c).

In this connection the stresses developed in the longitudinal sections were likewise calculated for the above moment of inertia and compared with the measured ones (Figure 2). A com-

parison of the two lines shows a satisfactory agreement.

The second series of tests, like the first, dealt with the bending about the vertical axis. The line of elastic deflection is shown in Figure 7. This line of deflection was likewise plotted, for the sake of comparison, along with the deflection line calculated for the total moment of inertia (Figure 7a). The difference between this deflection line and the measured one is approximately 1.12 times greater than in the case of the bending about the beam axis. This is due to the fact that the parts, which follow the assumed bending laws, participate to a smaller extent in the total moment of inertia than was the case for the bending about the beam axis. The deflection line, calculated by neglecting the side sheets, which work in compression, and the top and bottom sheets working in shear, agreed well with the measured one (Figure 7b). The deformation of the fuselage structure and of the covering and the stress distribution are quite similar to those considered in the case of the bending about the beam axis.

The third series of tests dealt with the torque of the fuselage. In this case particular stress was laid on exerting the moment in exactly the same way as is actually the case in practice. We can hardly speak of a rotation of the fuselage during these tests, but rather of its displacement caused by a moment exerted by the tail surfaces. When the force is exerted by the elevator, the fuselage is displaced according to Figure 8, the

right angles at the corners remaining unaltered and the two side walls sloping but very slightly. The measured angles  $\alpha'$  and  $\alpha''$  are shown in Figure 9. When, on the other hand, the moment is produced by the rudder, the fuselage shifts according to Figure 10 and bends about the vertical axis. On account of the difference between the height and width of the frame, the corresponding variations of the angles are larger than those produced by the action of the elevator.

The behavior of the sheet-metal covering is shown in Figures 8 and 10. The side sheet in each bay is affected along the field diagonals as shown by the arrows in Figure 8, and as indicated by the shadows on the affected sheet (Figure 11).

The behavior of the fuselage under the action of vibrations was investigated in connection with the static tests. Thereby the forced vibrations were produced by a device variable as to the direction and magnitude of the force and the number of revolutions (Figure 12), while the free vibrations were produced by a disengaging gear.

The vibrations were plotted directly or through a gear on a recording drum. For better comprehension, different phases of the vibration were photographed, after fitting to the end of the fuselage a lath likewise subjected to the action of the vibrations. A criterion of the vibration is thus obtained by the sharpness of the various parts of the lath in the photograph.

The first experiment consisted in the determination of the

resonance of the bending vibrations about the beam axis and the vertical axis in terms of the weight of the control surfaces. The test results and a vibration diagram are plotted as examples in Figures 13a and 13b. Figure 13a shows the calculated vibration numbers obtained on the assumption that, during the vibration, the deflection line practically coincides with the calculated line of the static tests, that there is a first fundamental vibration and a sinusoidal relation between the vibration and the time. Naturally the difference between the two periods of vibration decreases with increasing weight of the control surfaces.

The vibration about the vertical axis which, on account of the eccentric position of the control surfaces, is seldom quite pure, was produced in the present case by a shifting of the control weights.

During this test, the period of natural vibrations of the devices attached to the fuselage materially exceeded the resonance of the natural frequency of the fuselage. When there is only a slight difference between these two periods of vibration, the device vibrating in resonance causes the fuselage to adopt (on account of its not absolutely rigid fixation on the test stand) a length such that the fuselage likewise vibrates strongly at this period of vibration. Thus, on plotting the diagrams, there seem to be two resonance vibrations. A case quite similar to the one just described is also encountered in practice, when

the period of vibration of the control surfaces is similar to that of the fuselage. The investigation of the torsional vibrations chiefly dealt with the effect of the elevator.

When the two eccentrics in Figure 12 are staggered by 180 degrees, and a moment is thus exerted by the elevator on the fuselage, the latter will oscillate differently for different frequencies of excitation. As shown below, the different vibrations produced by the action of the same force are due to the fact that the axis of rotation of the power system does not coincide with the axis of rotation of the vibrating system.

The aforesaid types of fuselage vibration were determined for different moments of inertia of the elevator and for different weights. The motion of the fuselage end, as represented by the attached lath is shown in Figure 14 for a specific case. At 430 revolutions the vibration of the fuselage end causes the center of rotation to rise above the fuselage. The resulting deformation of the fuselage is represented by Figure 14a. On increasing the frequency of excitation, the fuselage passes through the resonance of the bending vibration about the vertical axis to a second torsional vibration, the center of rotation then lying at the bottom. The deformation of the fuselage under the action of this vibration is indicated by Figure 14b.

Free coupling vibrations were investigated in connection with these forced vibrations. Their behavior can be inferred

from what has been said above. The plotted bending vibration about the beam axis, coupled with a torsional vibration, is represented as an example in Figure 15.

Translation by W. L. Kaporinde, Paris Office,  
National Advisory Committee for Aeronautics.

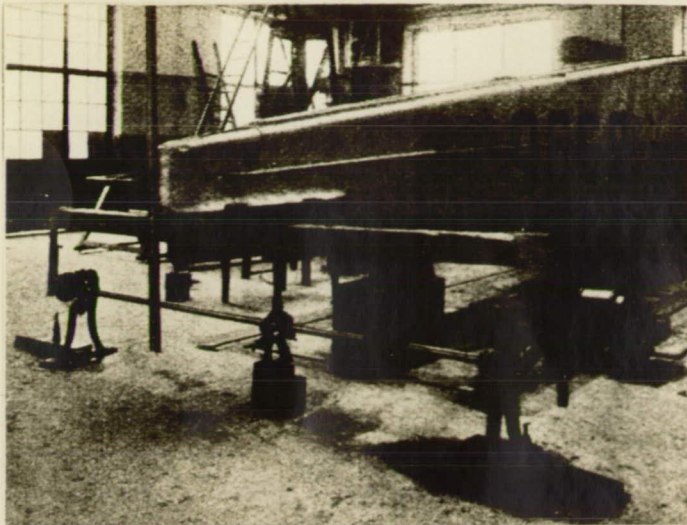


Fig. 12 Producing the fuselage vibrations

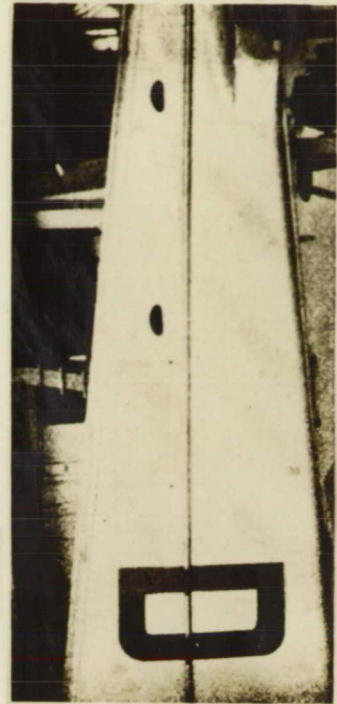


Fig. 11 Distortion of side sheet from torsional moment produced by elevator.

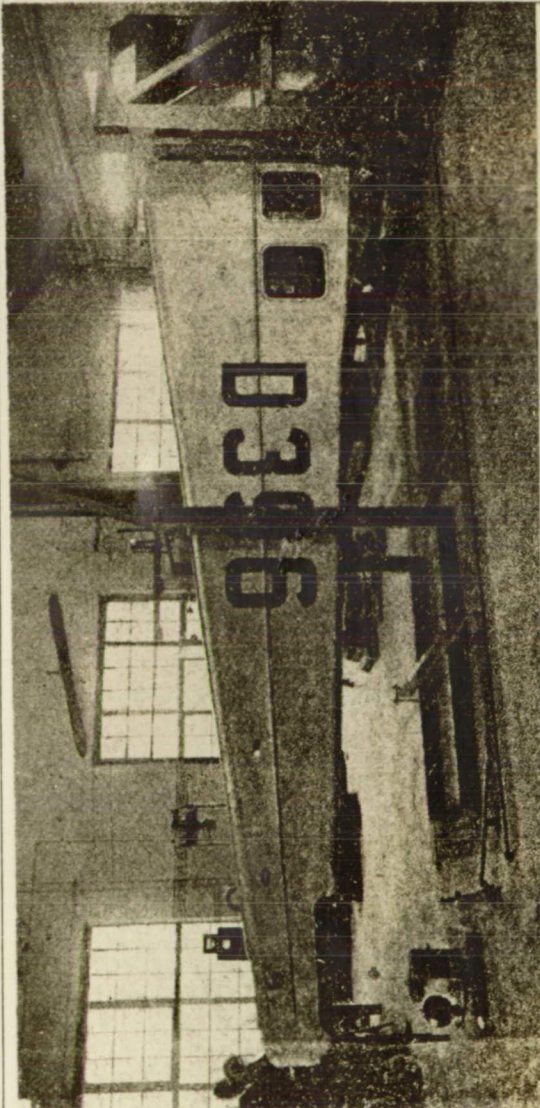


Fig. 1 Fuselage support.

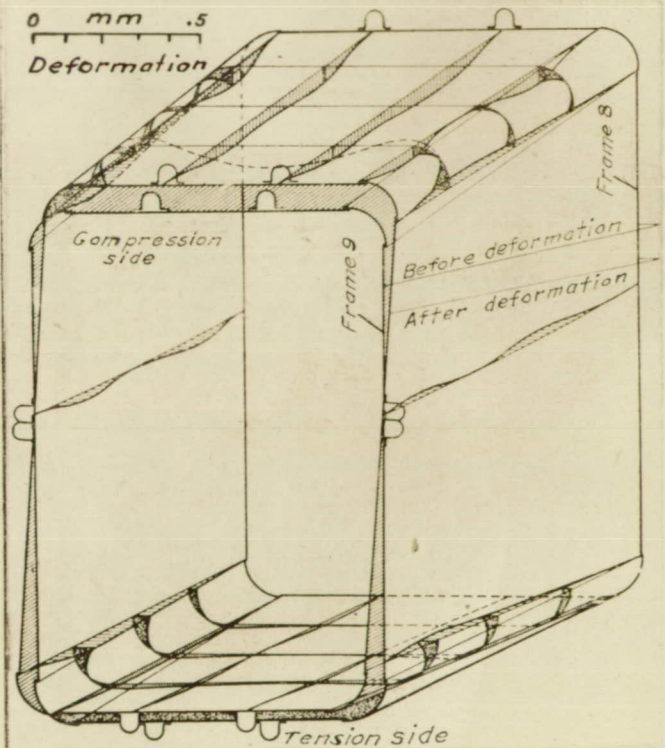
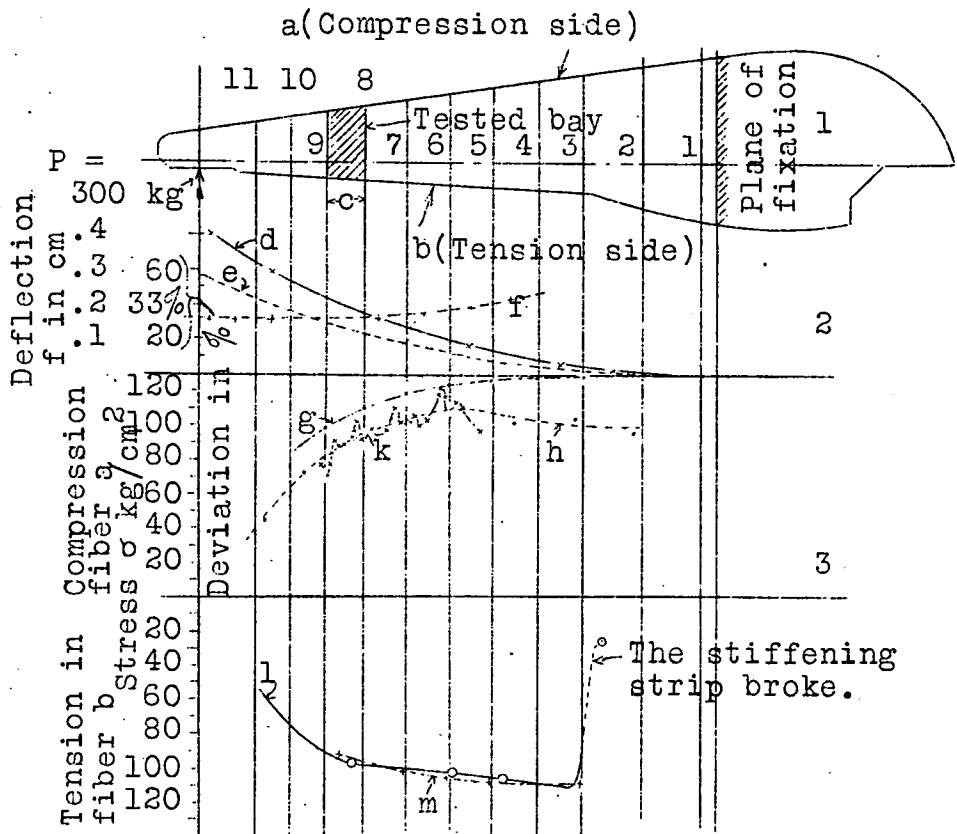


Fig. 3 Deformation of the tested bay for  $P = 300 \text{ kg (661.39 lb.)}$



- c Distance between frames
- d Measured
- e Calculated (inertia moment determined with whole cross section)
- f,  $\frac{f(\text{measured}) - f(\text{calculated})}{f(\text{measured})} \times 100$
- g Calculated compressive stress (inertia moment, determined without regard to the compressively stressed top metal sheet, and the lateral sheets introduced with half their value).
- h Mean measured compressive stress.
- k Measured compressive stress.
- l Measured tensile stress.
- m Calculated tensile stress (-)

Fig.2 Bending about the beam (horizontal) axis. Measured and calculated bending lines and stress distribution.

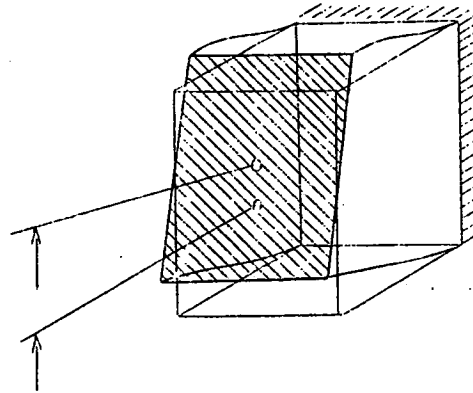
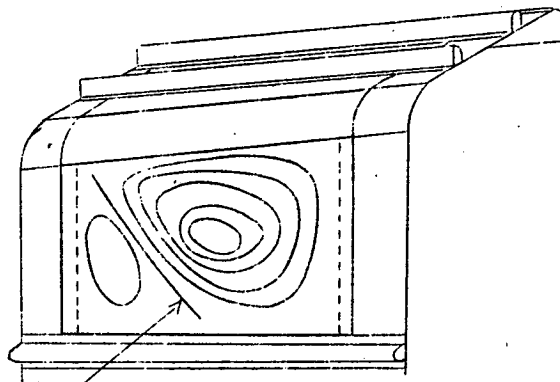
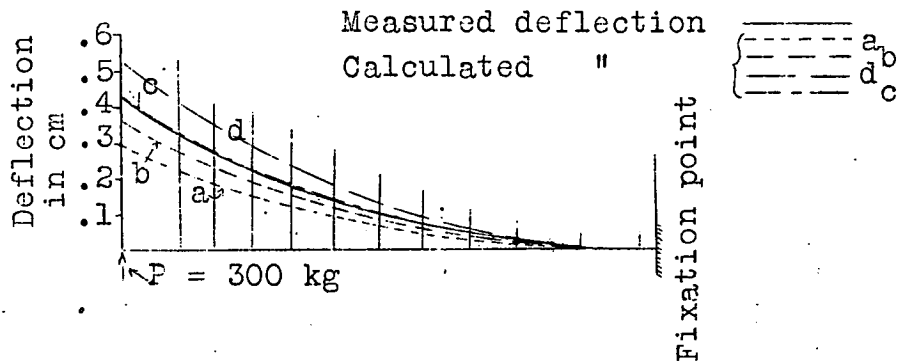


Fig.4 Deformation of bay without effect of covering.



Sheet-metal deflection=0

Fig.5 Lines of like bulge in one field in the bending about the horizontal or beam axis.



Calculation of inertia moment.

a With total cross section.

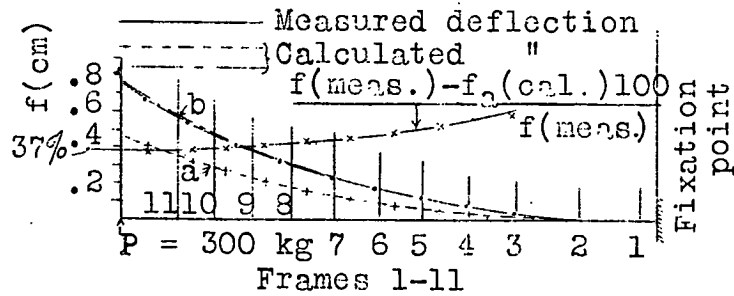
b Disregarding compressively stressed top sheet.

c " " " " " and half of the lateral sheets.

d Disregarding top sheet and lateral sheets.

Fig.6 Determination of fuselage inertia moment for the bending about the beam axis.

The lines of deflection calculated with various inertia moments.



a Inertia moment calculated with total cross section.  
 b Disregarding compressively stressed lateral sheets and the top and bottom sheets introduced with half their value.  
 Fig.7 Bending about the vertical axis.

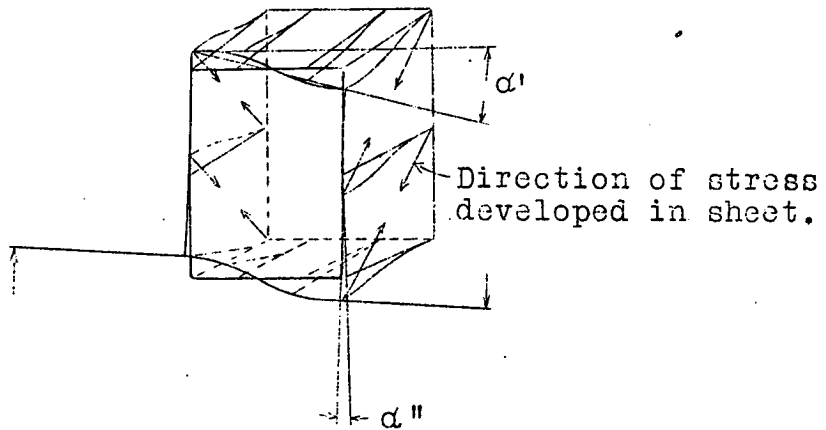


Fig.8 Deformation of fuselage from torsional moment produced by elevator.

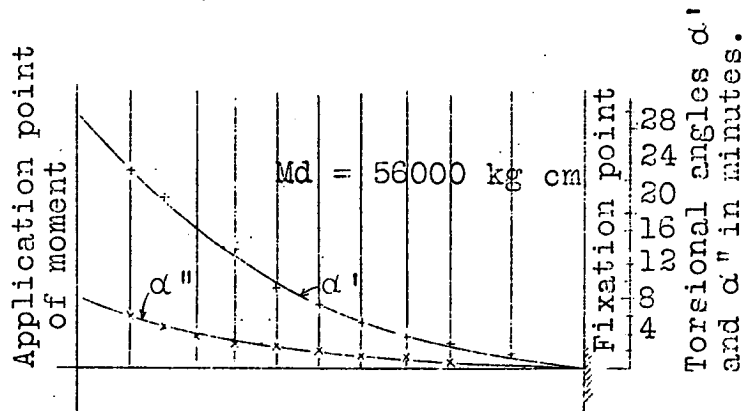


Fig.9 Inclination of top and bottom( $\alpha'$ ) and lateral parts ( $\alpha''$ ) of the frames from torsional moment produced by elevator.

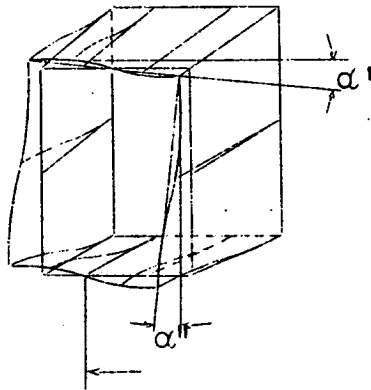


Fig.10 Deformation of fuselage from torsional moment produced by rudder.

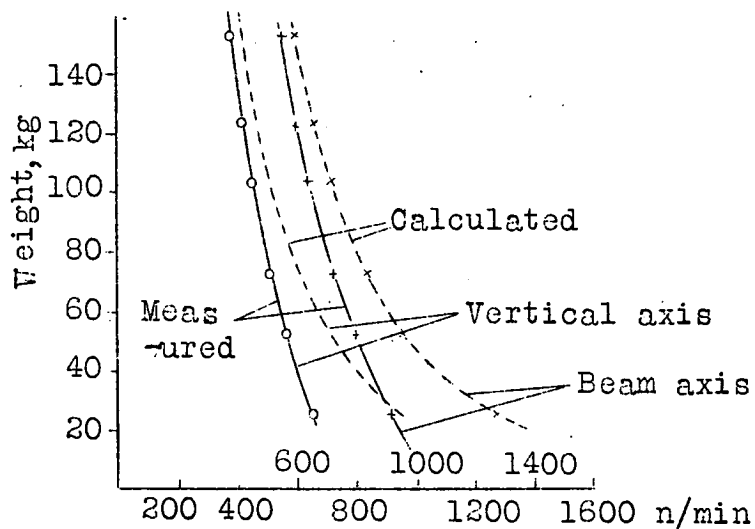


Fig.13a Vibration number about the beam and vertical axis for different weights of the control surfaces.

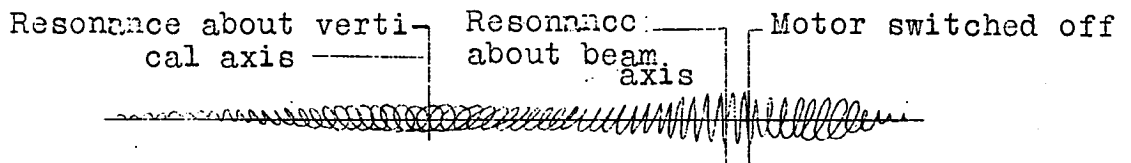
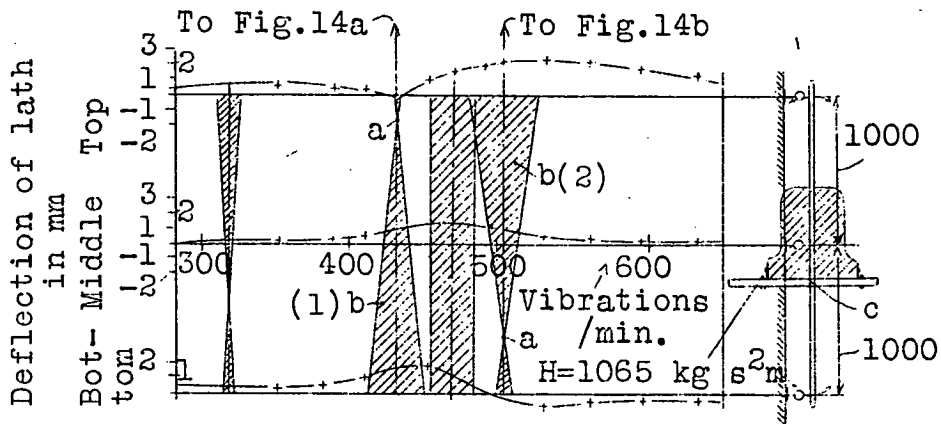


Fig.13b Recorded resonance about the beam and vertical axis.

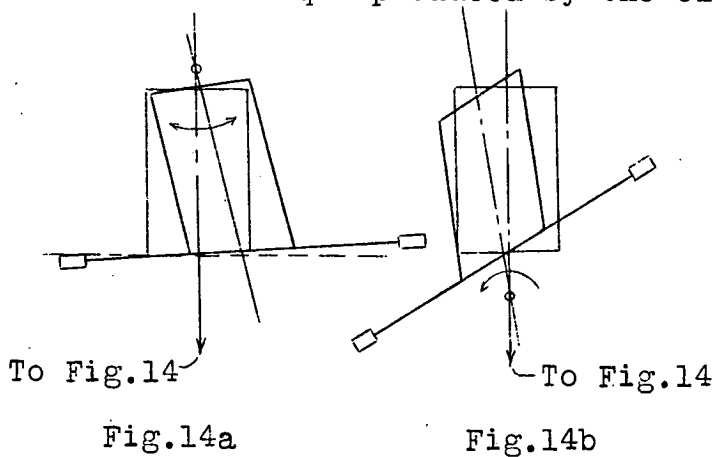


a Center of rotation.

b Resonance of torsional vibration.

c Reference axis for the inertia moments of the torsional vibrations.

Fig.14 Different kinds of fuselage vibrations in terms of the frequency for the variable torque produced by the elevator.



To Fig.14

To Fig.14

Fig.14a

Fig.14b

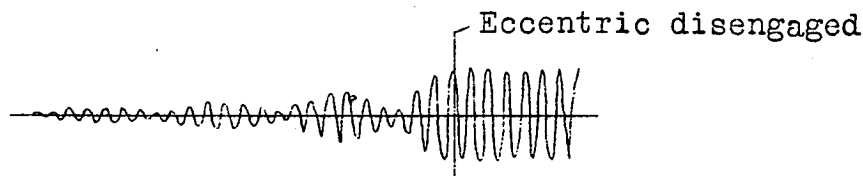


Fig.15 Record of coupled torsional bending vibrations.